Special aspects of reacting inviscid blunt body flow

Special aspects of reacting inviscid blunt body flow[1]

M. Fey, R. Jeltsch, P. Karmann

Research Report No. 92-07
July 1992

Seminar für Angewandte Mathematik
Eidgenössische Technische Hochschule
CH-8092 Zürich
Switzerland

[1]This research has been supported by the research and development program in the Hermes preparatory phase under contract RDANE 19/87 Step 3.

Special aspects of reacting inviscid blunt body flow

M. Fey, R. Jeltsch, P. Karmann

Seminar für Angewandte Mathematik
Eidgenössische Technische Hochschule
CH-8092 Zürich
Switzerland

Research Report No. 92-07 July 1992

Abstract

The problem of a hypersonic blunt body flow in two space dimensions is considered. The governing inhomogeneous Euler equations are given and the special treatment of calorically non-perfect gas in chemical non-equilibrium is described. The chemical model is given. The problem of the arising chemical boundary layer is discussed. Analytical and numerical investigations are used to analyse this boundary layer and to get error estimates for the numerical solution. Some modifications of the numerical method are given so that this boundary layer is indicated by the numerical solutions. An idea for a new boundary condition is proposed to obtain a better approximation of the wall pressure. Some two-dimensional test calculations are included.

Key words: chemical non equilibrium, boundary layer, numerical diffusion

Subject Classification: 35L65, 65M99, 76K05, 76N15

Introduction

In high temperature flow such as the reentry of a space vehicle the equations describing the fluid motion become inhomogeneous. For temperatures of 25000 K and Mach numbers of 25 as they arise in reentry, chemical reactions take place and depending on the geometry of the vehicle these reactions are not in equilibrium with the thermodynamical states.

In the following discussion the flow around a double ellipse with free stream Mach number of 25 and relatively low densities is numerically simulated (test case VI). In this case we assume thermodynamical equilibrium but include additional degrees of freedom for the particles so that the gas is no longer calorically perfect. The chemical reactions are in non-equilibrium. A finite volume approach with a body-fitted structured grid is used. Operator splitting is applied to separate the computations of the flow and of the chemical reactions. A low diffusion Van Leer flux vector splitting, proposed in [8], is used which is able to indicate the existing chemical boundary layer. The partial resolution of this extremely thin layer makes it possible to extrapolate the physical quantities from the flowfield to the surface of the body. This extrapolation is explained and could be used as a new boundary condition.

The governing equations

High temperature inviscid flows are described by the conservation equations for the partial densities of the different chemical species, the momentum and the total energy which can be written in two dimensions in the form

$$\frac{\partial U}{\partial t} + \frac{\partial F(U)}{\partial x} + \frac{\partial G(U)}{\partial y} = S(U) \tag{1}$$

where $U = (\rho_1, \ldots, \rho_N, m, n, E)^T$ is the vector of the conserved quantities and $S(U)$ denotes the source term due to chemical reactions. $F(U)$, $G(U)$ and $S(U)$ are the following column vectors

$$F(U) = \begin{pmatrix} \rho_1 \frac{m}{\rho} \\ \vdots \\ \rho_N \frac{m}{\rho} \\ \frac{m^2}{\rho} + p \\ \frac{mn}{\rho} \\ (E+p)\frac{m}{\rho} \end{pmatrix}, \quad G(U) = \begin{pmatrix} \rho_1 \frac{n}{\rho} \\ \vdots \\ \rho_N \frac{n}{\rho} \\ \frac{nm}{\rho} \\ \frac{n^2}{\rho} + p \\ (E+p)\frac{n}{\rho} \end{pmatrix}, \quad S(U) = \begin{pmatrix} s_1 \\ \vdots \\ s_N \\ 0 \\ 0 \\ 0 \end{pmatrix}.$$

The quantities $\rho_i,\ i = 1, \ldots, N$ denote the partial densities of the N different chemical species of the mixture, m and n are the momenta in x- and y-direction, E is the total energy per unit volume, $\rho = \sum_{i=1}^{N} \rho_i$ is the total density of the mixture, p is the pressure, $u = m/\rho$ and $v = n/\rho$ are the components of the fluid velocity and the terms s_i characterize the production of the ith species due to chemical reactions. In order to get a closed set of equations, the pressure p and the source term have to be related to the $N + 3$ components of U. The temperature can be obtained from the conservation equation for the total energy by an iteration method (e.g. Newton scheme). The pressure is given by the equation of state. The heat capacities are now functions of the temperature T and the mass fractions $Y_i = \rho_i/\rho$. The exact formulas and the evaluation of the flow properties are explained in detail in [7].

For the chemical reactions we use the five species model of air consisting of N_2,

O_2, N, O, NO with 17 reactions introduced by Park [15]. The reactions are

$$\left\{ \begin{array}{rcl} O_2 + M & \rightleftharpoons & 2O + M \\ N_2 + M & \rightleftharpoons & 2N + M \\ NO + M & \rightleftharpoons & N + O + M \\ NO + O & \rightleftharpoons & N + O_2 \\ O + N_2 & \rightleftharpoons & N + NO \end{array} \right\}$$

where M denotes a collision partner and is one of the five species. The source terms appearing in the equations are determined by the law of mass action described in [7].

Numerical scheme

The basic idea for solving the equation (1) is to split it into a system of ODEs for the partial densities and the homogeneous Euler equations. Note that during the first step, the integration of the system of ODEs

$$\frac{dU}{dt} = S(U),$$

the momentum, the total energy and the total density are constant. In the second step while solving the homogeneous Euler equations

$$\frac{\partial U}{\partial t} + \frac{\partial F(U)}{\partial x} + \frac{\partial G(U)}{\partial y} = 0 \tag{2}$$

the mass fractions stay constant. For the flow past the double ellipse the behavior of the chemical reactions within the flowfield was studied in detail (see [7], [9], [14]). There it has been shown that a simple Euler scheme is sufficiently accurate to solve the system of ODEs in the operator splitting procedure. For the present calculations an implicit Euler scheme is used for the chemical reactions.

Note that our operator splitting is quite different from the one used in [16] where the energy equation is not written in a homogeneous way and is therefore added to the chemical operator rather than to the gas dynamics operator. Moreover, we use an approach which is easier to extend to three-dimensional computations and complex geometries.

It is more difficult to obtain a solution to the homogeneous Euler equations (2). Due to the strong shock wave and the low density, most of the schemes were not able to capture this shock without unphysical values in the flowfield. We finally chose the Van Leer flux vector splitting method because no unphysical values appear during the computation. We modified the splitting so that real gas effects are included [18]. In [8] we reduced the number of contact discontinuities by using only the total density in the appearing Riemann problem. To keep the scheme as close to the physics as possible we use an exact contact surface for the partial densities. Hence the fluxes of the partial densities have been evaluated from the total density flux by

$$F_{\rho_i} = \left\{ \begin{array}{lll} Y_L^i \, F_\rho & \text{if} & F_\rho > 0 \\ Y_R^i \, F_\rho & \text{if} & F_\rho < 0 \end{array} \right. \tag{3}$$

where F_ρ is the total density flux and Y_L^i, Y_R^i are the mass fractions of species i from the left and right states of the Riemann problem. Computation showed that

there was a large increase of the total enthalpy in points where the gradients of the mass fractions of atomic nitrogen and oxygen are large. These results have been presented in [9].

In order to improve these results in [9] we treated the fluxes of the partial densities in the same way as the total density flux, that is

$$F_{\rho_i} = Y_L^i \; F_\rho^+ + Y_R^i \; F_\rho^- \tag{4}$$

where F_ρ^+ and F_ρ^- are the density fluxes in the positive and negative x-direction of the Van Leer flux vector splitting [13]. The variation of the total enthalpy was reduced to one third of the variation obtained with the first approach. Furthermore, the mass fractions of nitrogen and oxygen atoms decreased so that the temperature stayed constant as a result of this modification. In [8] it was shown that the flux in (4) is much more diffusive than the one in (3). The numerical diffusion of the standard Van Leer scheme reduces the mass fraction of nitrogen.

Since both flux formulas are not satisfactory, we want to combine their advantages. We use (3) for the fluxes of the partial densities to get a good approximation of the contact discontinuity in the partial densities. To introduce some control mechanism for the heat of formation in the energy equation and to have a low variation of total enthalpy in the steady state we use the fluxes from (4) multiplied by the formation enthalpy of the species. The energy flux F^E has therefore the form

$$F^E_{i+\frac{1}{2}} = F^{\tilde{E}}_{i+\frac{1}{2}} + \sum_{j=1}^{5} h_j^0 \hat{F}^\rho_{i+\frac{1}{2}} \tag{5}$$

where $F^{\tilde{E}}$ is the flux of Van Leer's scheme for a mixture of gases with no formation enthalpy. We call this scheme low diffusion Van Leer flux vector splitting (LDVL). The results are comparable to those computed by other "general purpose" methods given in the Proceedings of the Antibes Workshop Part I [5].

In order to better understand the error we used a totally different approach in [10], [12], [11]. In the case of a cylinder we obtain the solution of the steady reacting Euler equations along the stagnation point line by solving a two point boundary value problem (BVP) for a system of ordinary differential equations where a parameter function has to be taken from a two-dimensional calculation. With this approach we get a good approximation of the exact solution and Figure 1 shows that the LDVL scheme (5) is quite close to the solution even near critical points. In contrast to this, the standard Van Leer scheme (FVS, 4) shows only small gradients in the mass fractions near the stagnation point due to the large numerical diffusion.

Boundary Conditions

In the present calculations the boundary conditions are those of supersonic in- and outflow at all grid boundaries except the body. To obtain the pressure on the surface we connect the quantities in front of the body with a rarefaction wave to the state with normal velocity zero on the body.

In [10], [12], [11] we showed that there is a strong boundary layer for the desired body size due to the chemical reactions. Note that such chemical boundary layers have already been investigated by [2], [3], [4] and [17]. The difference to our analysis is pointed out in [12], [10], [11]. In [6] a hint is given that a chemical boundary layer is present. However the assumption of incompressibility at the stagnation point made in [6] seems to be incorrect. We could prove under very weak assumptions

that there is equilibrium in the stagnation point. But in the same analysis we also saw that this boundary layer is too thin to be a physical solution. From this point of view it would not be reasonable to force the chemical equilibrium at the boundary. However, numerical computations should give correct results of the mathematically formulated problem and thus the scheme should resolve the chemical boundary layer. In our calculations there are already some finite gradients visible near the stagnation point if we use LDVL even in a two dimensional calculation with rather coarse meshes compared to the boundary layer. The problem is to find good boundary values in this situation. For the simple cylinder we made a lot of calculations on various grids to examine the limiting behavior with decreasing cell size. In addition, we extrapolated the different quantities from the cell centers in the flowfield to the wall. We have found that except for pressure and velocity (normal and tangential) all quantities may have a boundary layer [12], [10], [11]. This has also been observed by the authors of [2], [3], [4] and [6]. In [17] a survey of older results concerning these boundary layers is given and a local analysis is done at the stagnation point. It is shown that the boundary layer of a quantity y has the form

$$y(x) = y_s + c(x_s - x)^{\alpha} \log^m(x - x_s)$$

where α is an eigenvalue of the Jacobian like matrix related to the chemical source term and m is a non-negative integer smaller than the multiplicity of this eigenvalue. Note that in [17] the chemical source terms are modeled differently than in this paper. For our extrapolation we use the somewhat more simplified ansatz:

$$y(x) = y_s + c(x_s - x)^{\alpha} \tag{6}$$

The parameters y_s, c and α can be either fitted using the three nearest points or calculated from a nonlinear least square problem to reduce the influence of the errors due to boundary conditions. Both methods give almost the same results.

The most sensitive variable is the temperature. There are three possibilities to calculate this temperature. First, we extrapolate the temperature directly. Secondly, we extrapolate the conserved quantities $\rho_1, ..., \rho_N$ and E and set the normal velocity to zero. Then we calculate the temperature (called T_E) and get the pressure p_E from the equation of state. The gradient of the energy may be infinite but we know that the pressure gradient is zero in x_s [12]. Therefore, as the third posibility, we take the pressure in front of the wall, the extrapolated partial densities and use the equation of state to calculate the temperature T_p.

For this investigation we have done five test calculations for a flow past a cylinder of radius 0.1 m. The cell size decreases from 0.5 mm to 0.1 mm in steps of 0.1 mm. Table 1 shows the behavior of the different temperatures at the stagnation point. In the columns T_1 and p_1 we added the values of temperature and pressure in the first cell next to the boundary. We find that with decreasing cell size the boundary layer is more and more resolved. Even in the case of the coarsest mesh we can reduce the temperature by 350 K to 8159 K with our extrapolation method.O n the finest mesh we get 7780 K. More interesting in view of the boundary condition is the pressure (see Table 1). Here the results are quite surprising. For the cylinder the pressure in the flowfield increases to 2100 Pa while refining the grid. On the other hand the value obtained by using the extrapolated variables is decreasing to 2074 Pa. The corresponding value obtained from the BVP is 2061 Pa. This seems to indicate that the mesh sizes used are still not small enough to exhibit convergence of the non-extrapolated values of the pressure, while the extrapolated wall values converge. One should note that the stand-off distance depends in a very sensitive way on the wall pressure and therefore these differences can be of importance.

Using this investigations we can in principle construct a new boundary condition.

Table 1: temperature and pressure for different mesh sizes (smallest cell).

h	T	T_E	T_p	T_1	p_1	p_E
0.5	8198.80	8159.02	8215.18	8509.97	2090.68	2076.39
0.4	8116.70	8077.29	8144.92	8427.06	2091.53	2075.94
0.3	8023.47	7984.80	8040.98	8331.90	2094.21	2075.66
0.2	7940.61	7903.77	7971.03	8249.37	2096.29	2074.52
0.1	7811.18	7780.11	7860.46	8116.63	2099.16	2073.65

For the velocity on the surface we take the velocity of the first cell next to the boundary and set its normal component to zero. Then we extrapolate the partial densities and total energy in the direction normal to the surface using ansatz (6). Finally we calculate the pressure p_E at the wall from these extrapolated quantities.

Numerical results and conclusions

The geometry and the free stream conditions for our calculations are taken from the specifications of the Workshop on Hypersonic Reentry Problems [1], Part II. The testcase VI is considered here. We use a grid with 313 points along the body and 85 points normal to it. The mesh is refined near the body to resolve the chemical boundary layer. In order to be able to compare the quality of resolution of this boundary layer by a discretization, one should compare the numerical results in relation to the cell size at the surface. In our case the smallest cell at the body surface is 0.18 mm times 0.73 mm. Figures 2 – 5 show the quantities next to the body and Figures 6 – 10 show contour plots of the whole flowfield. These results are obtained with the expansion wave as boundary condition.

The values at the stagnation point propagate along the surface and due to the low temperature and pressure away from this point the species concentrations freeze and the mass fractions should be constant. On the other hand the velocity normal to the wall is almost zero and so the fluxes normal to the wall are in the "subsonic mode". Nevertheless the computed values of the mass fractions are nearly constant demonstrating the low diffusion of the scheme (see Figure 3).

To get an idea of the influence of the new boundary condition we extrapolate the values at the surface using ansatz (6). This condition can not be applied to all boundary points and even if the extrapolation gives a result, it is very sensitive to small disturbances in the flowfield. In Figures 11 and 12 the results obtained with the old (C1) and new (C2) boundary conditions are compared. The temperature and pressure decreases near the stagnation point while the density and mass fraction of nitrogen atoms increase. Our investigations in [12] suggest that the values of the second approach may be better. Nevertheless this procedure is not usable for real applications because of the strong sensitivity shown in the figures. We also do not know in which way this kind of boundary conditions influences the flowfield.

References

[1] *Book of Abstracts of the Workshop on Hyperbolic Flows for Reenry Problems, Part*

II, April 15 – 19, 1991, volume 4, 1991.

[2] Raul J. Conti. Stagnation equilibrium layer in nonequilibrium blunt body flow. *AIAA J.*, 2:2044–2046, 1964.

[3] Raul J. Conti. A theoretical study of non-equilibrium blunt body flow. *J. Fluid Mech.*, 24(1):65–88, 1966.

[4] Raul J. Conti and Milton Van Dyke. Reacting flow as an example of a boundary layer under singular external conditions. *J. Fluid. Mech.*, 38(3):513–535, 1969.

[5] J.-A. Désidéri, R. Glowinski, and J. Périaux, editors. *Hypersonic Flows for Reentry Problems, Proceedings of the Workshop held in Antibes, France, 22-25 January, 1990*, volume 2. Springer Verlag, 1992.

[6] Jean-Antoine Désidéri. Some comments on the numerical computations of reacting flows over the double-ellipse (double ellipsoid). In [5], volume 2, 1992.

[7] Michael Fey, Helmut Jarausch, Rolf Jeltsch, and Peter Karmann. On the Interaction of Euler and ODE Solver when Computing Reactive Gas Flow. In J. E. Flaherty, P. J. Paslow, M. S. Shephard, and J. D. Vasilakis, editors, *Proceedings of the Workshop on Adaptive Computational Methods for Partial Differential Equations*. SIAM, 1988.

[8] Michael Fey and Rolf Jeltsch. Influence of numerical diffusion in high temperature flow. In I. L. Rhyming, editor, *Proceedings of the 9th GAMM Conference on Numerical Methods in Fluid Dynamics, Notes on Numerical Fluid Mechanics*. Vieweg Verlag, 1992.

[9] Michael Fey, Rolf Jeltsch, and Peter Karmann. Numerical analysis of chemically reacting inviscid flow in 2-d. In [5], 1992.

[10] Michael Fey, Rolf Jeltsch, and Siegfried Müller. The influence of a source term, an example: chemical reacting hypersonic flow. In A. Donato, editor, *Proceedings of the 4th International Conference on Hyperbolic Problems, Taormina 1992*. Vieweg Verlag. to appear.

[11] Michael Fey, Rolf Jeltsch, and Siegfried Müller. Stagnation point computations of non-equilibrium inviscid blunt body flow. *Computers & Fluids*. to appear.

[12] Michael Fey, Rolf Jeltsch, and Siegfried Müller. *Stagnation Point Analysis*. Research Report No. 92-03, Seminar für Angewandte Mathematik, ETH Zürich, 1992.

[13] Bram van Leer. Flux-vector splitting for the Euler equations. *Lecture Notes in Physics*, 170:507–512, 1982.

[14] Vera Montag. Analyse verschiedener lösungsalgorithmen für differentialgleichungssysteme chemischer reaktionen. Master's thesis, RWTH Aachen, 1990.

[15] Chul Park. On convergence of computation of chemically reacting flows. Technical Report 085-0247, AIAA, 1985.

[16] M. Valorani, M. Onofri, B. Favini, and F. Sabetta. Nonequilibrium hypersonic inviscid steady flows. *AIAA J.*, 30(1):86–93, 1992.

[17] Marcel Vinokur. On stagnation point conditions in non-equilibrium inviscid blunt body flows. *J. Fluid. Mech.*, 30:49–75, 1970.

[18] Helen Yee. Upwind and symmetric shock-capturing schemes. Technical Report TM 89464, NASA, 1987.

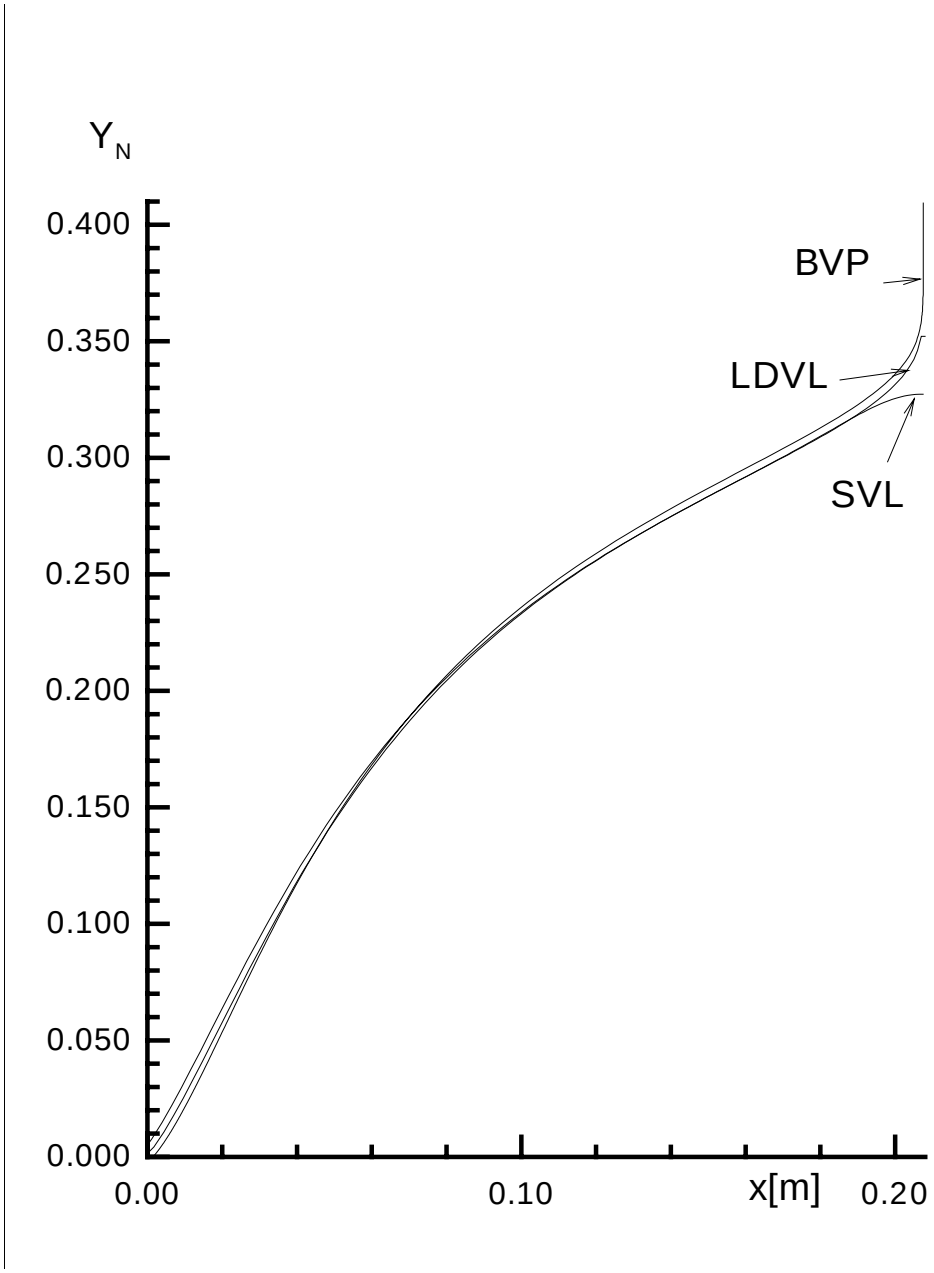

Figure 1: DIFFERENT SOLUTIONS AT THE STAGNATION POINT LINE. (BVP) BOUNDARY VALUE PROBLEM, (SVL) STANDARD VAN LEER, (LDVL) LOW DIFFUSION VAN LEER.

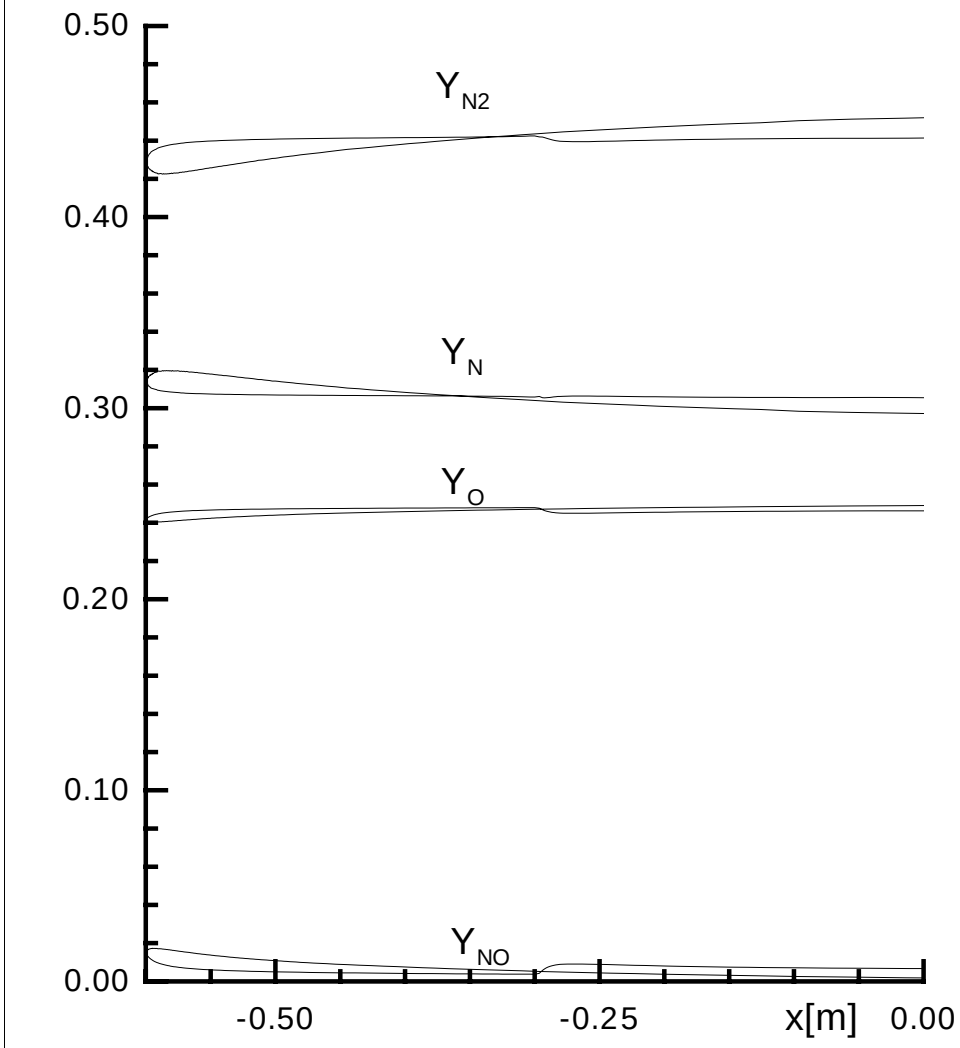

Figure 2: MASS FRACTIONS AT THE WALL

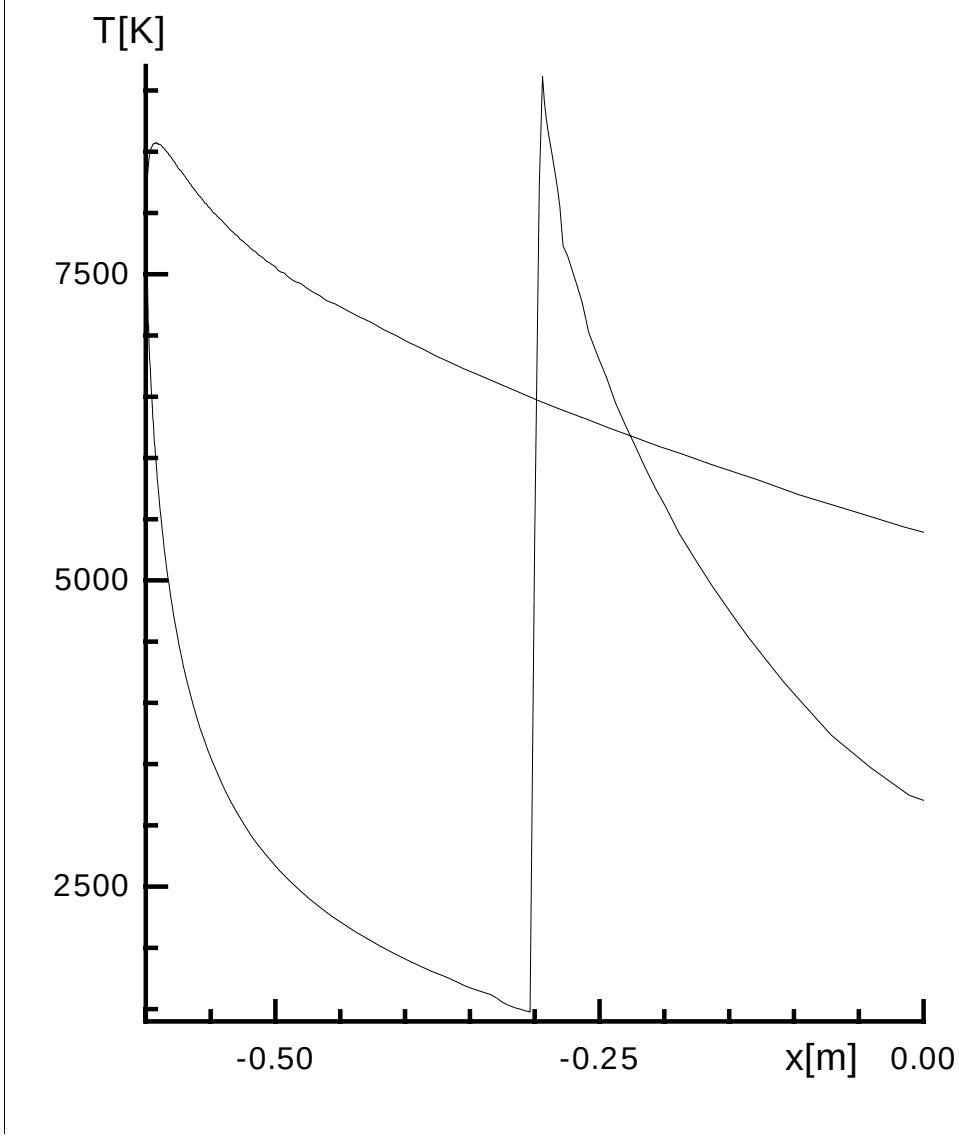

Figure 3: TEMPERATURE AT THE WALL

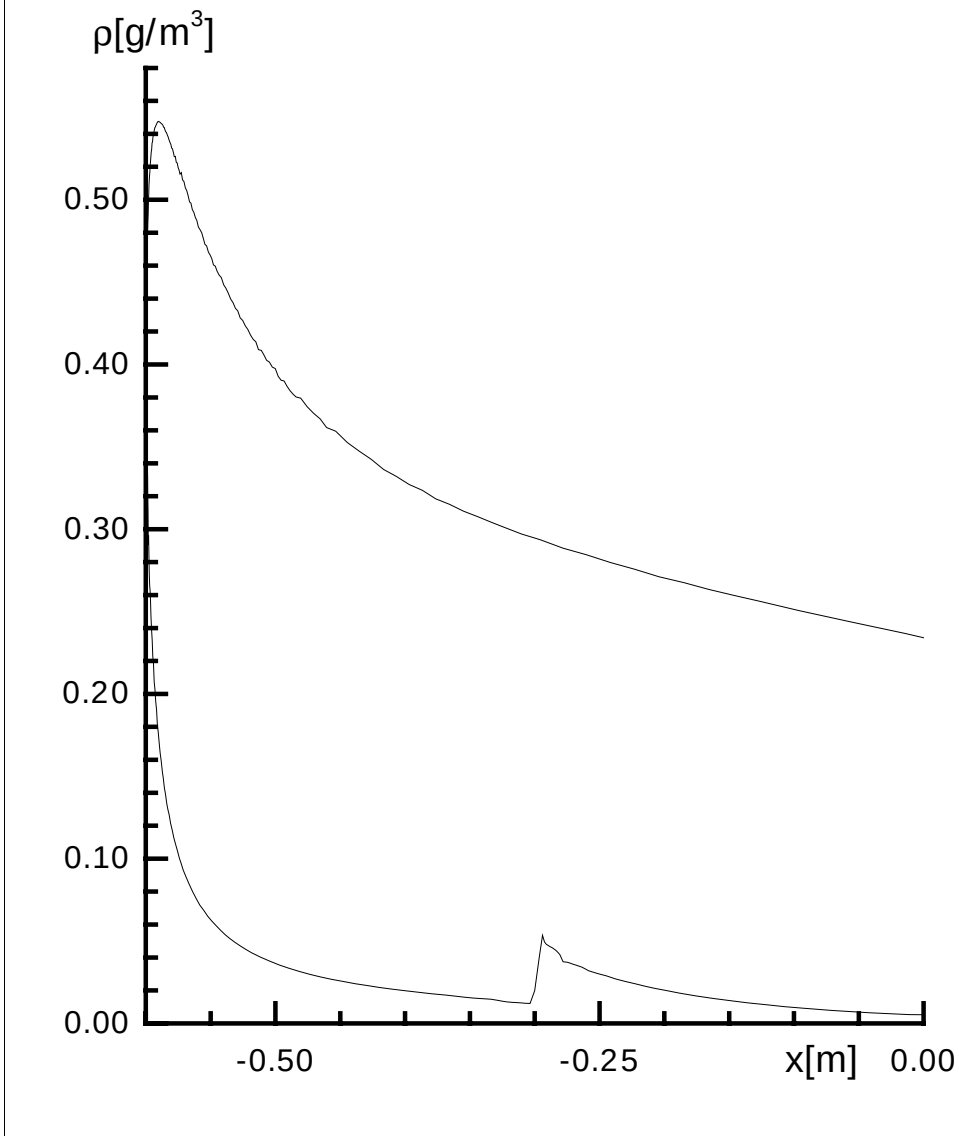

Figure 4: DENSITY AT THE WALL

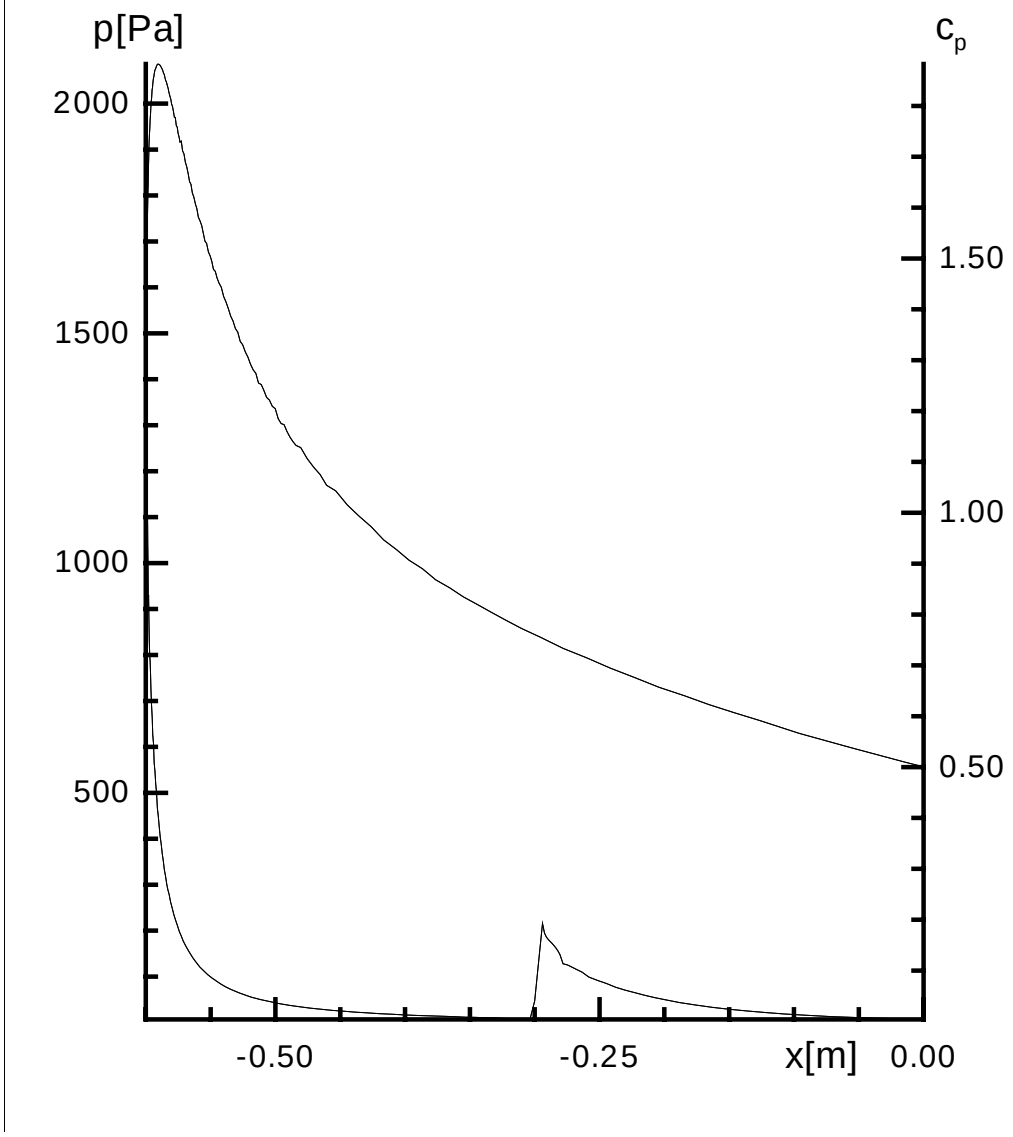

Figure 5: PRESSURE AT THE WALL

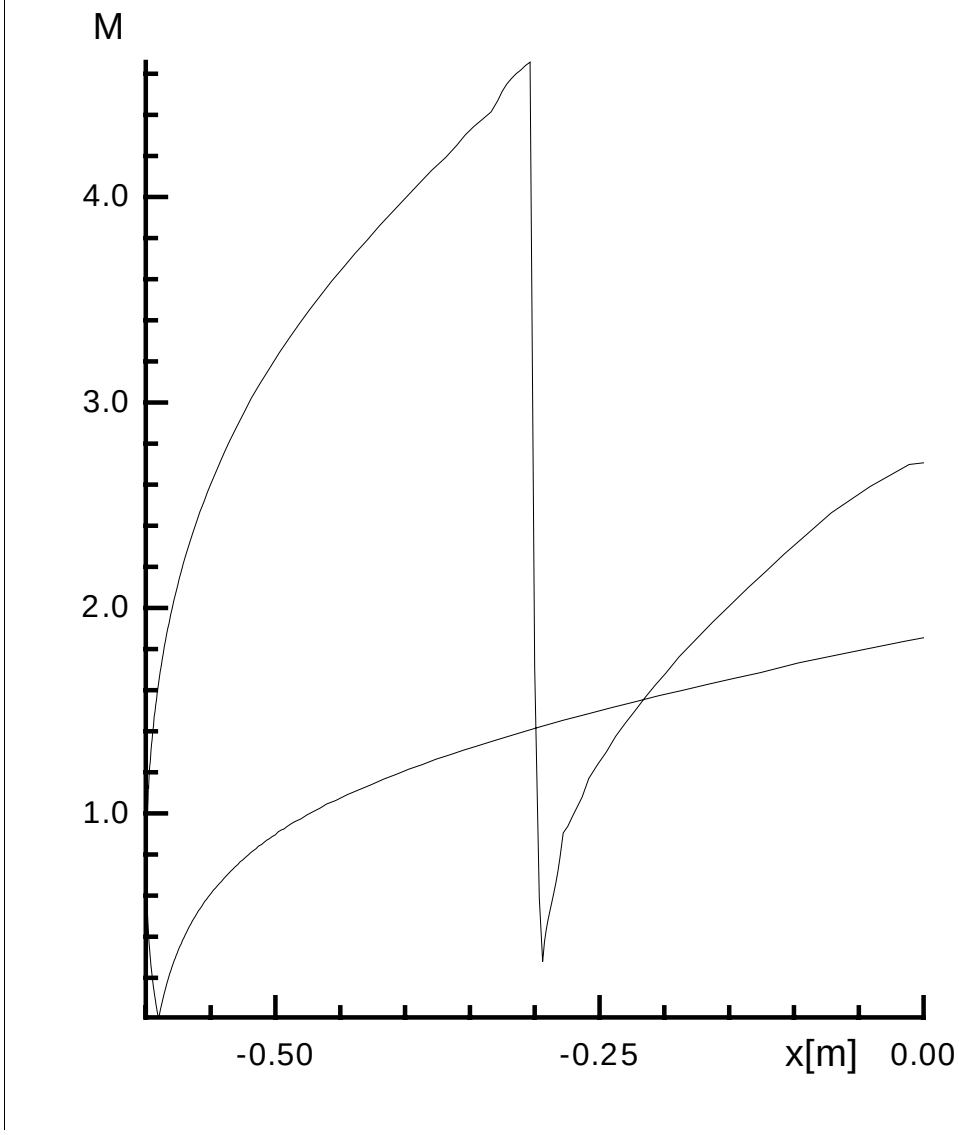

Figure 6: MACH NUMBER AT THE WALL

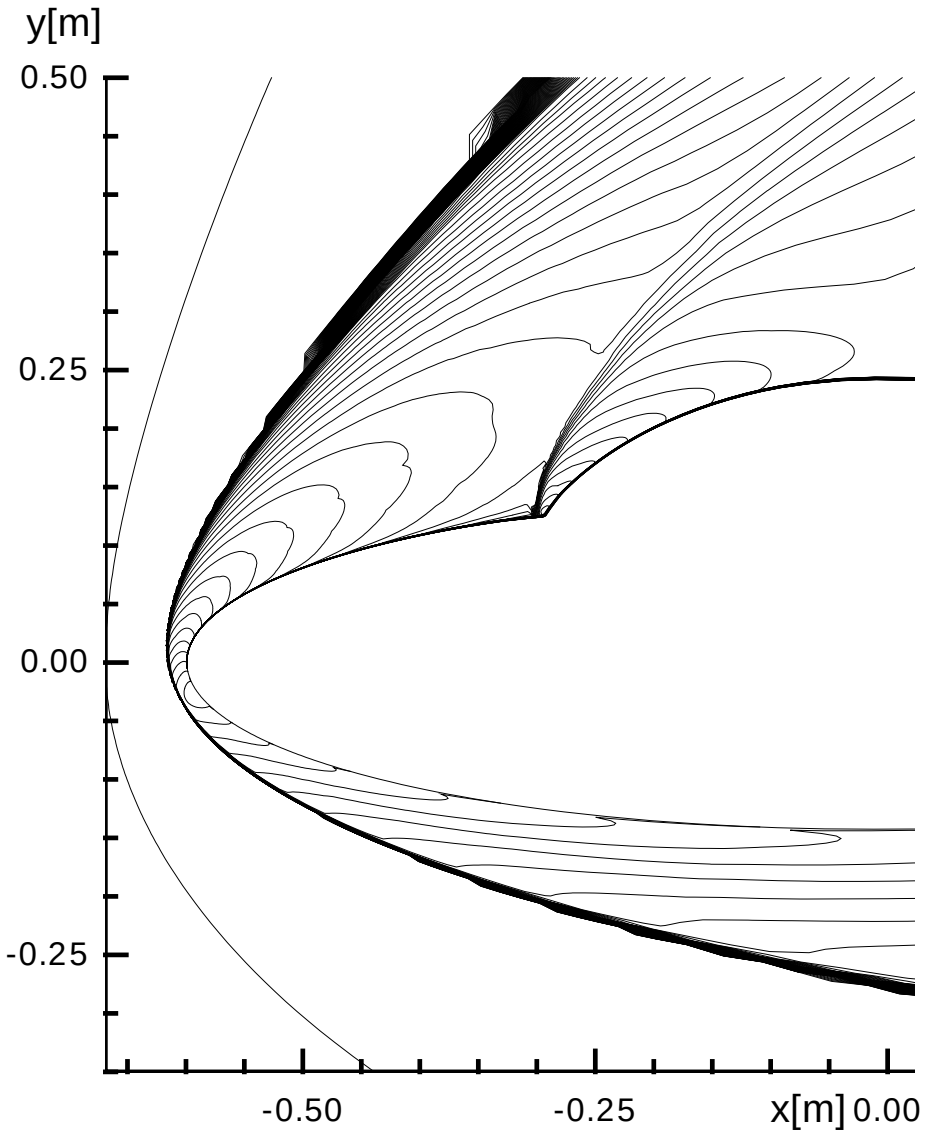

Figure 7: MACH NUMBER CONTOURS ΔM = 0.25

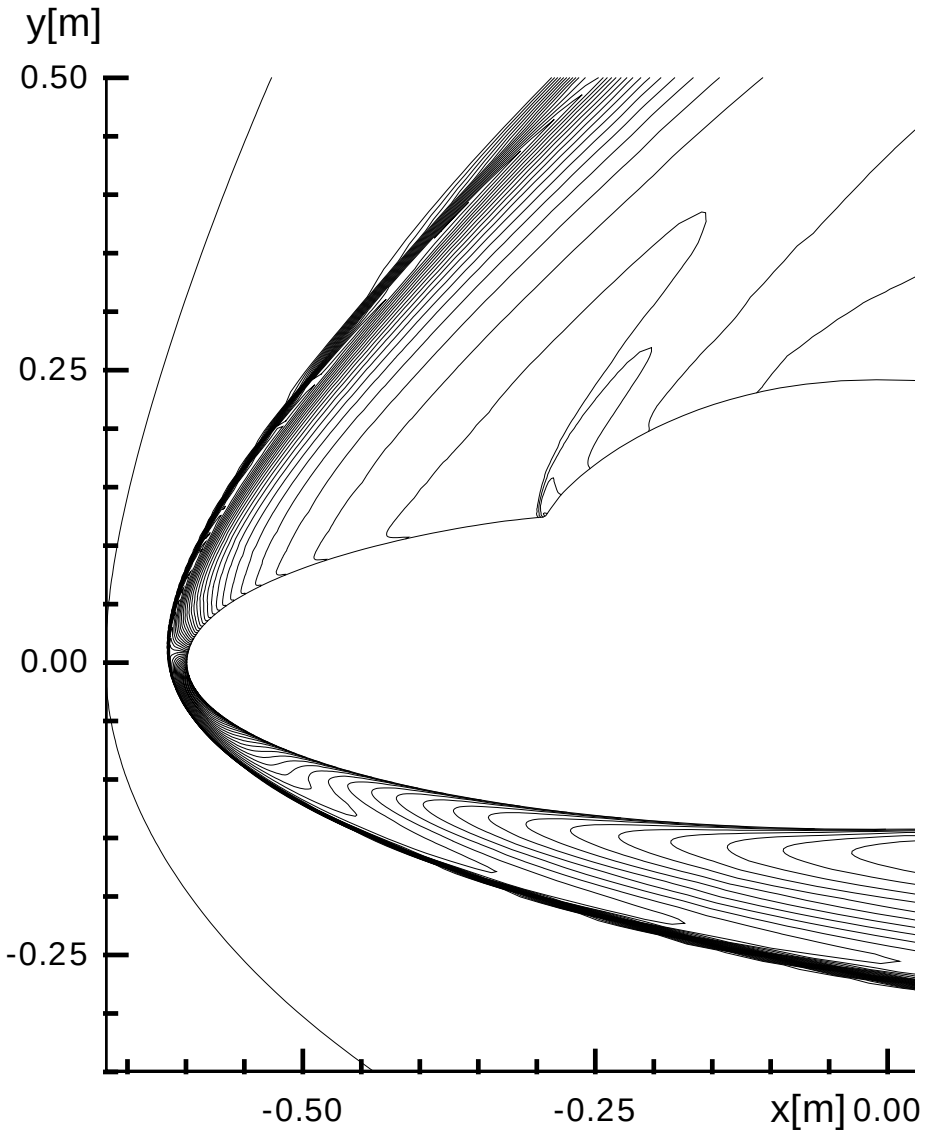

Figure 8: DENSITY CONTOURS $\Delta(\rho/\rho_\infty) = 0.25$

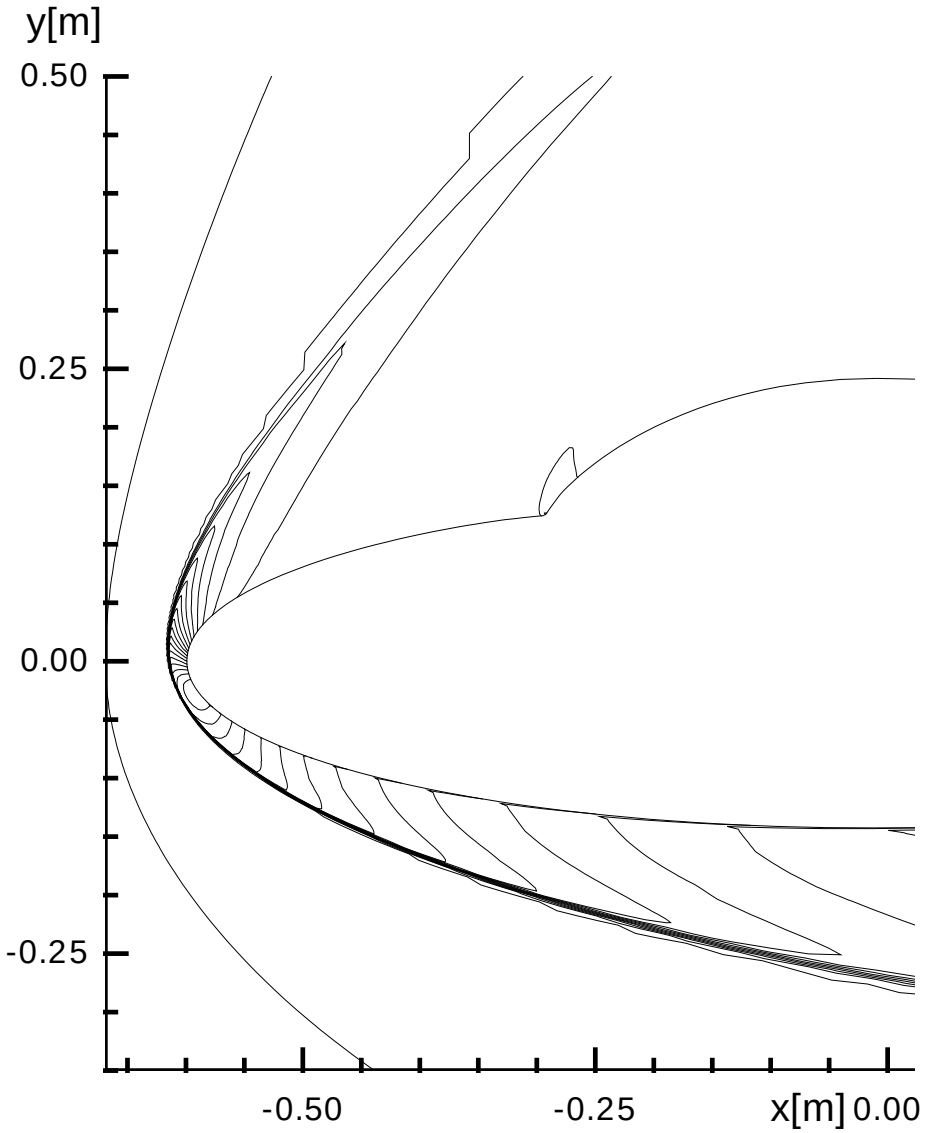

Figure 9: PRESSURE CONTOURS $\Delta C_p = 0.25$

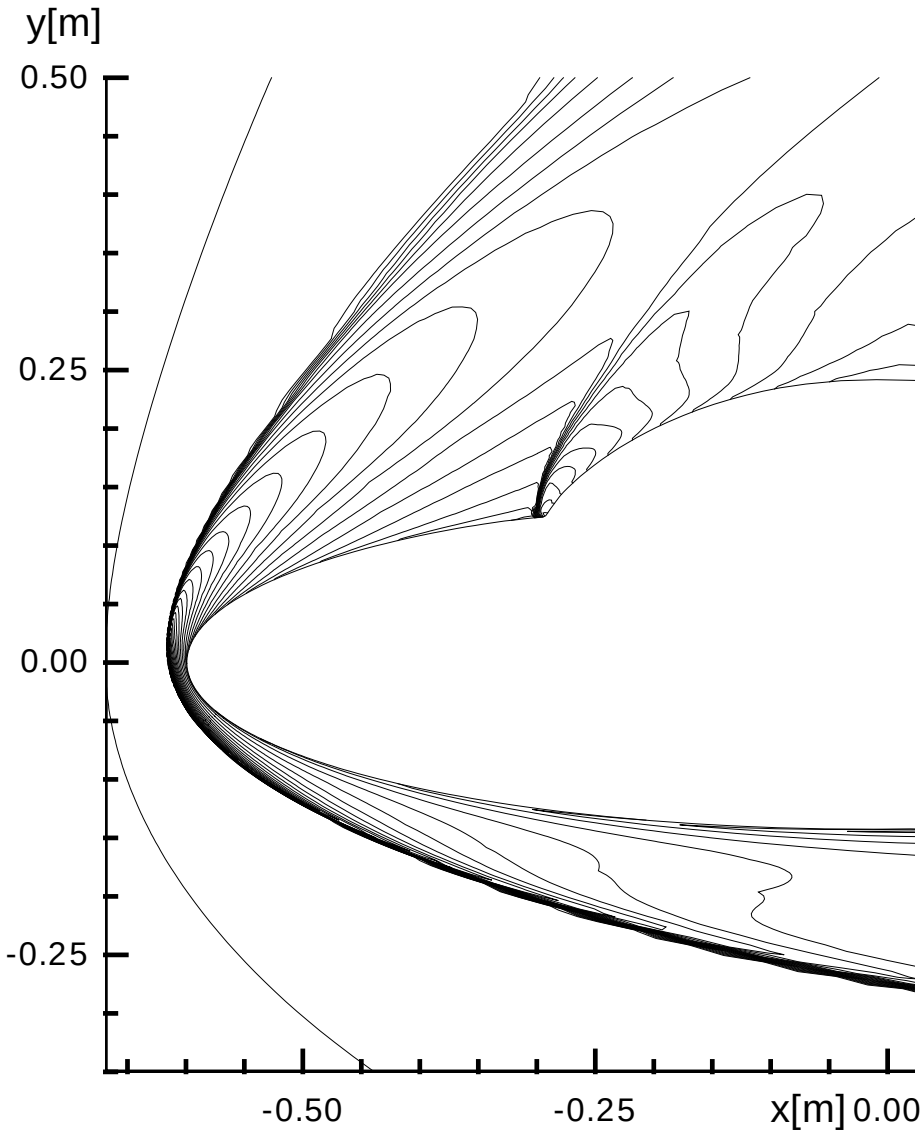

Figure 10: TEMPERATURE CONTOURS $\Delta T = 0.25$

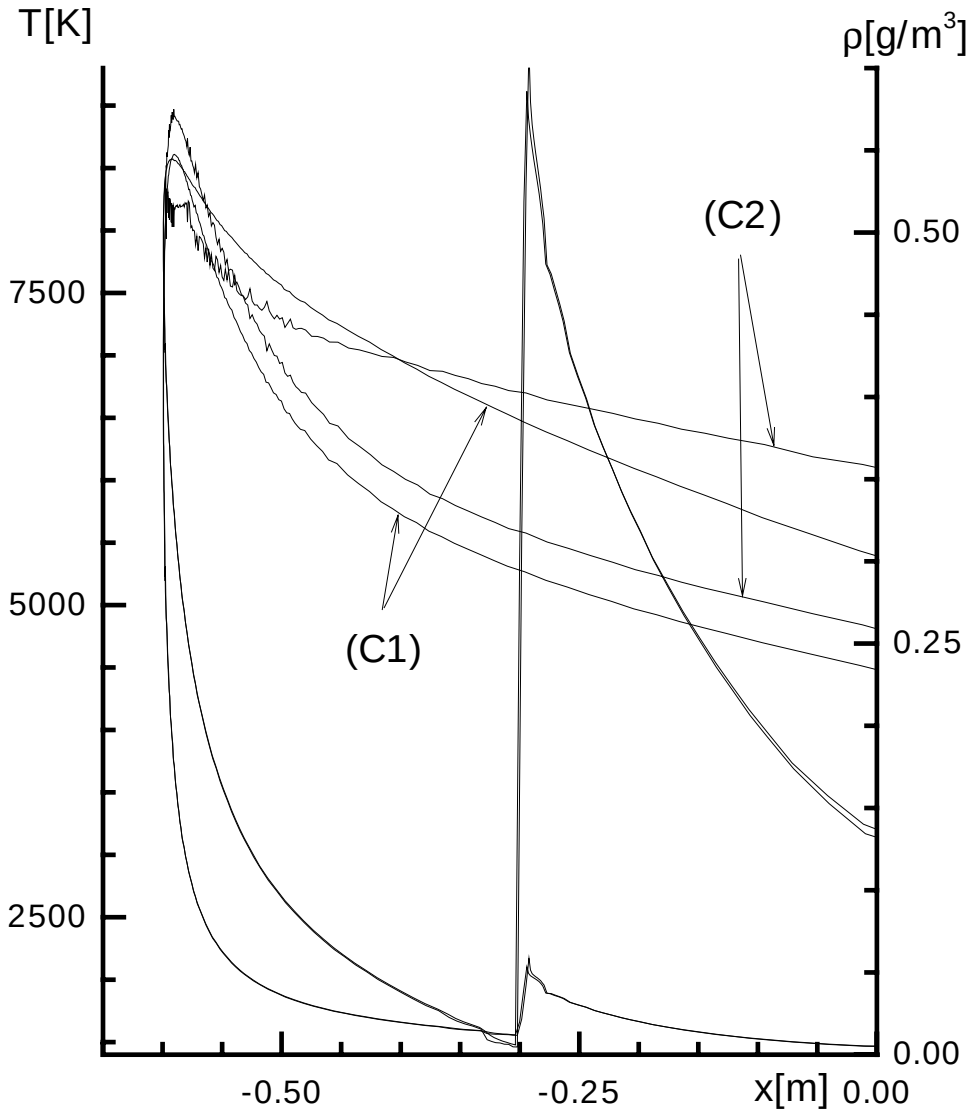

Figure 11: COMPARISON OF TEMPERATURE AND DENSITY AT THE WALL FOR TWO DIFFERENT BOUNDARY CONDITIONS

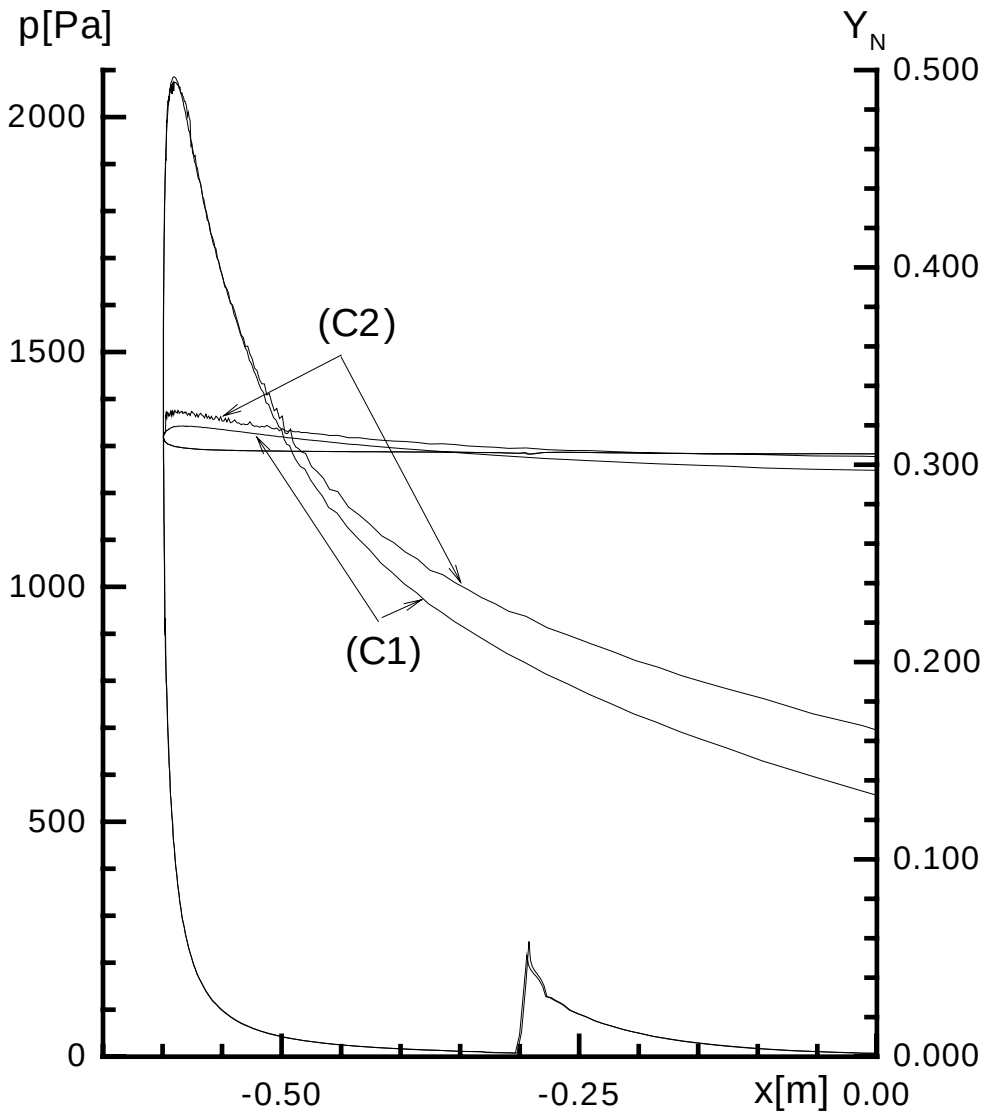

Figure 12: COMPARISON OF PRESSURE AND MASS FRACTION AT THE WALL FOR TWO DIFFERENT BOUNDARY CONDITIONS

Research Reports

No.	Authors	Title
92-07	M. Fey, R. Jeltsch, P. Karmann	Special aspects of reacting inviscid blunt body flow
92-06	M. Fey, R. Jeltsch, S. Müller	The influence of a source term, an example: chemically reacting hypersonic flow
92-05	N. Botta, J. Sesterhenn	Deficiencies in the numerical computation of nozzle flow
92-04	Ch. Lubich	Integration of stiff mechanical systems by Runge-Kutta methods
92-03	M. Fey, R. Jeltsch, S. Müller	Stagnation point analysis
92-02	C. W. Schulz-Rinne, J. P. Collins, H. M. Glaz	Numerical Solution of the Riemann Problem for Two-Dimensional Gas Dynamics
92-01	R. J. LeVeque, K. M. Shyue	Shock Tracking Based on High Resolution Wave Propagation Methods
91-10	M. Fey, R. Jeltsch	Influence of numerical diffusion in high temperature flow
91-09	R. J. LeVeque, R. Walder	Grid Alignment Effects and Rotated Methods for Computing Complex Flows in Astrophysics
91-08	Ch. Lubich, R. Schneider	Time discretization of parabolic boundary integral equations
91-07	M. Pirovino	On the Definition of Nonlinear Stability for Numerical Methods
91-06	Ch. Lubich, A. Ostermann	Runge-Kutta Methods for Parabolic Equations and Convolution Quadrature
91-05	C. W. Schulz-Rinne	Classification of the Riemann Problem for Two-Dimensional Gas Dynamics
91-04	R. Jeltsch, J. H. Smit	Accuracy Barriers of Three Time Level Difference Schemes for Hyperbolic Equations
91-03	I. Vecchi	Concentration-cancellation and Hardy spaces
91-02	R. Jeltsch, B. Pohl	Waveform Relaxation with Overlapping Splittings